NEW EXPERIMENTS IN MARTIAN IMPACT VAPOR-INDUCED WIND STREAK ANALYSIS. S. N. Quintana[1], P. H. Schultz[1], and S. S. Horowitz[2], [1]Brown University Department of Earth, Environmental, and Planetary Sciences, 324 Brook Street, Providence, RI 02912, stephanie_quintana@brown.edu, [2]NeuroPop, Inc.

Introduction: On Mars, impact-related wind streaks are visible only in nighttime infrared [1-3]. We propose that impact-generated vapor couples to the atmosphere as it expands, and it displaces the entire atmospheric column. From previous computational simulations, the winds that result from this process can reach tornadic speeds and above, which can entrain very fine dust (<0.001 mm) and material greater than 100 mm in size [4-5]. Surface material entrained in impact-induced winds can substantially scour the surface, especially when the flow interacts with preexisting obstacles, such as craters and ridges [5]. The scars left by winds remain semi-permanent on the surface. The latest experiments on impact vapor-induced winds test impacts into layered targets, impacts from volatile projectiles, and different atmospheric compositions.

Previous Work: Both computational simulations and impact experiments support the hypothesis that the enigmatic, thermally bright wind streaks observed around some craters on Mars result from intense, impact vapor-induced winds. Models and experiments explore the process of vapor generation in order to explain the relative paucity of these 'vapor-wind streaks' on Mars. The streaks may be the result of near-surface volatiles, an easily mobilized surface layer, or the characteristics of the impactor itself.

CTH models. 2D and 3D computational simulations carried out with the CTH shock physics analysis package [6] help to inform the physical processes that develop in the laboratory and allow us to test planetary-scale events under a variety of conditions. Such simulations tested the effect of target composition, impactor composition, and atmospheric conditions on the development of vapor and high-speed winds on Mars [2]. The 45° collision of a dunite impactor into a basaltic surface overlain by a surface volatile layer enhanced the development of a vapor plume compared to the 'control' case (the same impact into a solid basaltic crust). While the impact of a volatile 'comet' into a solid basaltic crust produced a smaller crater and less vaporization than the impact into the volatile layer, enough vapor was generated to induce winds and vortices downrange. Both models demonstrate the importance of target and impactor composition on the development of strong impact generated winds. Ongoing models, combined with crater surveys of Mars further explore these effects [7, this volume].

Experiments. Experiments at the Ames Vertical Gun Range (AVGR) allow for the exploration of wind development and its connection to other impact processes including shockwaves and vapor expansion. High-speed cameras and a slew of instruments recorded three separate phenomena resulting from Pyrex projectile impacting a powdered dolomite target in the presence of a ~30 mbar atmosphere of air [3]. Cameras first captured a surface roughening that spreads supersonically away from the impact point. Based on the speed and symmetry, this roughening is attributed to the air-coupled shockwave generated at the atmosphere/target boundary at the point of first contact. A separate, ground-coupled shockwave was recorded by geophones attached to the side of the target container. Finally, the cameras documented the development of winds, as expressed by streamers of powdered dolomite blowing off of dusty pipe cleaners placed near the target edge. On Earth, the blast wave is the concurrent expansion of the air-coupled shockwave together with strong wind [8]. Yet the laboratory experiments under a reduced atmospheric pressure demonstrate that sustained winds begin well after the passage of the air-coupled shockwave.

Although it appears that the winds must be due to the impact-vapor coupling to the ambient atmosphere, additional experiments were performed in order to demonstrate this distinction more clearly. Our strategy is to assess the effects of the degree of vaporization and ambient atmospheres.

New Experiments: New experiments at the AVGR tested the effects of atmosphere composition (and thus density), as well as the effects of a layered target and a volatile (polyethylene) impactor. As before, each shot entered the chamber to a ~30 mbar atmosphere, but the new experiments tested helium and argon atmospheres instead of air. In order to test the effect of a layered target on vapor production, layers of pumice 3-12 mm thick were placed over the powdered dolomite target. Pumice does not vaporize easily at laboratory impact speeds of 4-6 km/s, and thus suppressed vapor formation upon impact.

A variety of sensors installed within the large impact chamber recorded various aspects of the impact process. Geophones placed along the sides of the target container recorded ground-related shock effects. Additionally, microphones and vertical stacks of pressure sensors placed ~45 cm from the target center both uprange and downrange recorded air-related effects. Sunlamps inside the impact chamber that usually illuminate the target sufficiently for the high-speed cam-

eras were not used due to instrument sensitivity; hence, no data could be gathered from the cameras on the air-coupled shockwave or wind development.

Results: The latest set of experiments more clearly separate the air-coupled shock effects from the vapor expansion in different atmosphere compositions. A suite of experiments from 30°-90° under both a helium atmosphere and an argon one provided comparisons with previous shots into air. Fig. 1 depicts the average speed of the atmospheric disturbance for each angle in argon (a) and helium (b). For air-coupled shocks, we expect that a 90° impact angle will produce a symmetric shockwave that travels at approximately the speed of sound. Because 90° impacts generate a signal on the pressure sensors that is nearly consistent with the speed of sound in each of the ambient gases, the detected atmospheric disturbance that the pressure sensors detect is indeed the air-coupled shockwave, not the result of vapor expansion or winds. The faster shock speeds downrange for impacts below 90° are the result of the added downrange momentum from the impactor.

Even though the sunlamps remained off during each impact, for tens to hundreds of microseconds, impact products were self-luminous, which allowed for the cameras to record several frames during the process. The suppression of impact-induced vaporization could be visualized with the addition of a layer of pumice over the more easily vaporized dolomite powder. Comparisons demonstrate the difference in vapor production and high-speed downrange ejecta between a 45° impact into a 3 mm (Fig. 2a) and 12 mm (Fig. 2b) layer of pumice (both in an argon atmosphere). The 12 mm thick layer of pumice suppresses much of the high-speed, downrange moving vapor, except in the case of a volatile (polyethylene) impactor. In that case, low-angle vapor derived mostly from the projectile travels downrange at high speed while a self-luminescent vapor trail follows down the projectile wake.

Conclusions: Laboratory experiments demonstrated that impacts into an easily volatilized material under laboratory conditions can induce strong winds. These types of winds are suspected to be the source of crater-related wind streaks that are found around some martian craters, primarily visible in thermal infrared. Here, we demonstrated the distinction between the shockwave generated at the first moment of impact and potential winds generated by impact vaporization by using non-volatile surface layers with different thicknesses and different atmospheric compositions (affecting the speed of sound). These results provide the basis for more detailed 3D computational models that will help to resolve the origin of impact-generated winds, their implications for surface preservation, and possibly the nature of the impacting bodies.

Acknowledgements: We thank the crew of the AVGR, without whom these experiments would be impossible. This material is based upon work supported by the National Science Foundation Graduate Research Fellowship, Grant No. DGE- 1058262 and the NASA Mars Fundamental Research Program (MFRP), Grant No. NNX13AG43G.

References: [1] Schultz, P. H. and Quintana, S. (2013), *LPSC 44*, Abstract #2697. [2] Quintana, S.N. and Schultz, P.H. (2014), *LPSC 45*, Abstract #1971. [3] Quintana, S.N., et al. (2015), *LPSC 46*, Abstract #2469. [4] Iversen et al. 1976, *Icarus* **29**, 381-393. [5] Greeley, R. and Iversen, J.D. (1985), Cambridge Univ. Press. [6] McGlaun, J.M. et al., (1990), *Int'l J. of Impact Eng.*, *10*(1-4), 351-360. [7] Quintana, S.N. and Schultz, P.H. (2016), *LPSC 47*, Abstract #1548. [8] Glasstone, S. and Dolan, P.J. (1977), United States DOD and DOE.

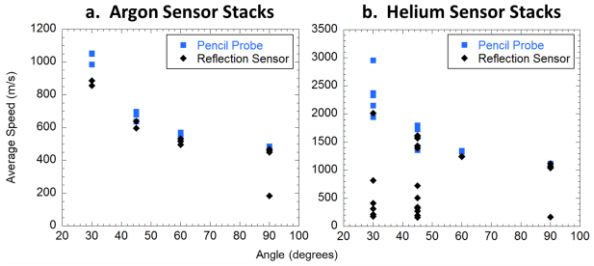

Figure 1 – Average speed vs. impact angle of pressure wave in the atmosphere, (a) Ar and (b) He, recorded from downrange sensor stacks.

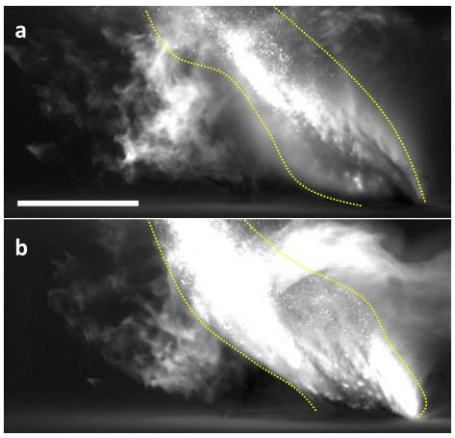

Figure 2 – Comparison of a 45° impact (left to right) into a (a) 3 mm and (b) 12 mm layer of pumice over dolomite showing increased vapor suppression in (b). Scale bar is 5 cm. Dotted yellow line denotes high-speed ejecta. Turbulent pattern in front of the curtain (at left) and entrainment of ejecta (diffuse component) represent self-luminous the vapor generated at impact.